Chaotic Modeling and Simulation (CMSIM) 1: 3–16, 2020

Turbulence in Space Plasmas on Magnetohydrodynamic and Kinetic Scales

Wiesław M. Macek[1,2]

[1] Faculty of Mathematics and Natural Sciences
Cardinal Stefan Wyszyński University
Wóycickiego 1/3, 01-938 Warsaw, Poland
[2] Space Research Centre, Polish Academy of Sciences
Bartycka 18 A, 00-716 Warsaw, Poland
(E-mail: macek@cbk.waw.pl)

Abstract. Turbulence is a complex behavior that remains a challenge for contemporary science. Space plasmas can be considered natural laboratories for investigating the complex dynamics. We have produced phenomenological models for turbulence in solar wind plasmas on large-(inertial) magnetohydrodynamic scales, based on observations by the *Voyager* in the heliosphere and *THEMIS* missions in the Earth's magnetosheath, where timescales are usually shorter than those in the heliosheath. However, to understand the physical mechanisms governing turbulence in the space plasma environments, it is necessary to investigate the experimental data on even much smaller scale lengths. Therefore, we have considered turbulence using observations from the *Magnetospheric Multiscale* (*MMS*) mission on kinetic (ions and electron) scales, which are far shorter than the scales characteristic for description of plasma by magnetohydrodynamic (MHD) theory. It is worth noting that the unprecedented very high millisecond-resolution of the magnetic field instrument enabled us to analyze turbulence on scale lengths of only tens of kilometers, i.e. extremely small in space. In particular, it has appeared that a clear break of the magnetic spectral exponent to about -11/2 at frequencies 20 – 25 Hz agrees with the predictions of kinetic theory (-16/3). Hence we can hope that the results of these investigations can facilitate a better understanding of the physical mechanisms of turbulence.
Keywords: Turbulence, Space plasmas, Magnetohydrodynamics, Kinetic theory.

1 Introduction: Importance of Turbulence

Turbulence is a complex phenomenon that still remains a challenge for contemporary physics [11,4]. Notwithstanding great progress in magnetohydrodynamic (MHD, Hall-MHD, two-fluid) simulations, the physical mechanisms for turbulence are still not clearly understood. Turbulent magnetic fields play an important role in plasmas, e.g. leading to magnetic reconnection [33,7,3,29,30,10] and the redistribution of kinetic and magnetic energy in the space environments and laboratory plasmas. Reconnection occurs when the

Received: 10 July 2019 / Accepted: 24 November 2019

ISSN 2241-0503

electrons cannot supply the current needed to support antiparallel magnetic fields. The dynamic variability of plasma and fields at very small electron scales in the solar system is not well known.

However, collisionless space and astrophysical plasmas can be considered natural laboratories for investigating the complex dynamics [6]. In particular, the solar wind is a stream of charged particles (mainly ions and electrons) flowing from the Sun with the embedded magnetic field; this plasma of solar origin fills-up the Solar System, including the magnetosheath surrounding the terrestrial magnetosphere. Moreover, reconnection processes may play an important role in mixing heliospheric and interstellar plasmas, as postulated in Ref. [15], a hypothesis supported by numerical simulations [27,28]. Reconnection at the heliopause, which is the ultimate boundary separating the heliosphere from the very local interstellar medium, has yet to be confirmed by experimental data.

Solar wind plasma turbulence based on various space missions has been extensively studied within the European Community's FP7 project in collaboration with the European scientific institutions, as depicted in Fig. 1. In Section 2 we provide an example of the results obtained using Voyager data. The second part of the paper is devoted to magnetospheric turbulence based on *THEMIS* data, Section 4, and especially *Magnetospheric Multiscale* (*MMS*) mission with data, methods, and results in the magnetosheath discussed in the respective Sections 5, 6, and 7. The conclusions of solar wind and magnetospheric turbulence are summarized in Sections 3 and 8, respectively.

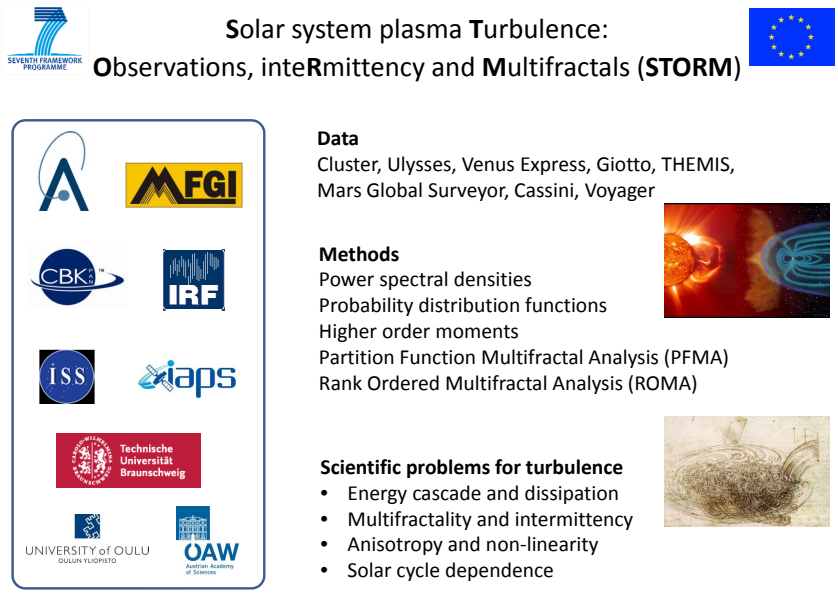

Fig. 1. Data, methods, and scientific problems for turbulence in STORM project.

2 Solar Wind Turbulence

Our previous studies have produced phenomenological models for turbulence including a weighted two-scale Cantor set model [16,18]. We have applied this model to solar wind turbulence in solar wind plasmas on large-(inertial) magnetohydrodynamic scales, based on observations by the *Voyager* in the entire heliosphere [19,21,22] and even at the heliospheric boundaries [20].

2.1 Multifractal Spectrum

In particular, using our multifractal model [16], which is a convenient tool to investigate multifractality, we have confirmed the characteristic shape of the multifractal singularity spectrum, $f(\alpha)$, which is a downward concave function of scaling indices α, see Ref. [9].

2.2 Degree of Multifractality

The universal function $f(\alpha)$ provides the information about the distribution of the generalized dimensions D_q over various scales [25]. In particular, for a monofractal behavior this function is reduced to a single point D_0 (for $q = 0$), a fractal capacity dimension. Therefore, the width of this function $\Delta \equiv \alpha_{\max} - \alpha_{\min} = D_{-\infty} - D_{\infty}$ is called the degree of multifractality [16,19], and is used as a measure of intermittency, cf. [11].

2.3 Analysis of Voyager Data in the Heliosphere

For example, the multifractal spectrum $f(\alpha)$ is calculated for the weighted two-scale (continuous lines) model and the usual one-scale (dashed lines) p-model [24] with the parameters fitted using the magnetic fields (diamonds) measured by Voyager 1 in the heliosheath at various distances before crossing the heliopause, (a) 94–97 AU, (b) 105–107 AU, (c) 108–111 AU, and (d) 112–115 AU, respectively as shown in Fig. 2, cf. [20].

2.4 Multifractal Turbulence at the Heliospheric Boundaries

The values of the degree of multifractality Δ in the heliosphere versus the heliospheric distances compared to a periodically decreasing function (dotted) during solar minimum (MIN) and solar maximum (MAX), declining (DEC) and rising (RIS) phases of solar cycles, with the corresponding averages shown by continuous lines are shown in Fig. 3. The crossing of the termination shock (TS) and the heliopause (HP) by Voyager 1 are marked by vertical dashed lines. Below is shown the Sunspot Number (SSN) during years 1980–2010, cf. [21,22].

We see that the degree of multifractality of magnetic field fluctuations embedded the solar wind plasma decreases slowly with the heliospheric distance, demonstrating that this quantity is still modulated by the solar cycles further in the heliosheath, and even in the vicinity of the heliopause, possibly approaching a uniform non-intermittent behavior in the nearby interstellar medium, which could be interesting for astrophysicists.

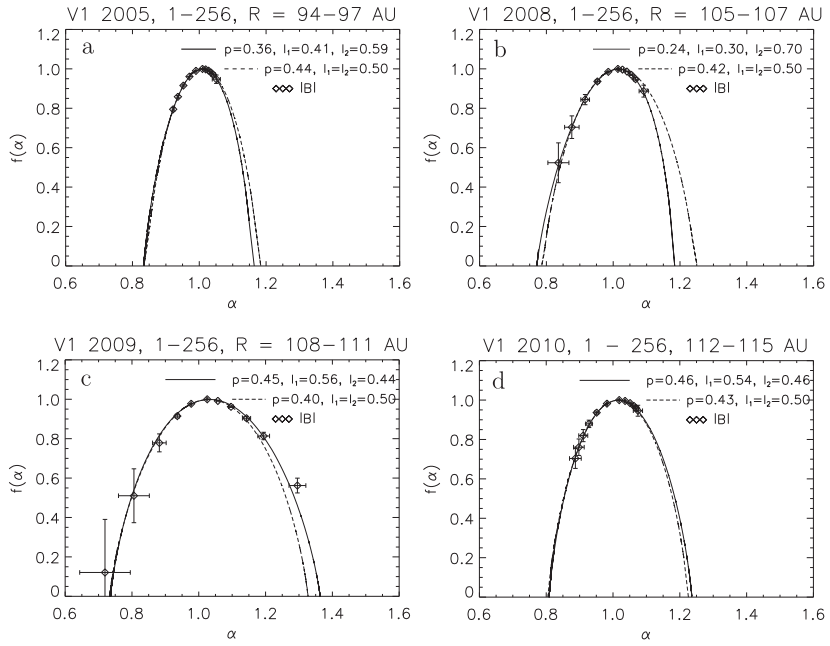

Fig. 2. The singularity spectrum $f(\alpha)$ as a function of a singularity strength α.

3 Solar Wind Conclusions

We have identified the scaling region of fluctuations of the interplanetary magnetic field. In fact, using our two-scale model based on the weighted Cantor set, we have examined the universal multifractal spectra before and after crossing by Voyager 1 the termination shock at 94 AU and before crossing the heliopause at distances of about 122 AU from the Sun.

We have shown that the degree of multifractality Δ for magnetic field fluctuations of the solar wind falls steadily with the distance from the Sun and seems to be modulated by the solar activity.

We have provided an important evidence that the large-scale magnetic field fluctuations reveal the multifractal structure not only in the outer heliosphere, but in the entire heliosheath, even near the heliopause. In our view, any accurate physical model must reproduce the multifractal spectra. In particular, the non-multifractal scaling observed after the heliopause crossing suggests a non-intermittent behavior in the nearby interstellar medium, consistent with the smoothly varying interstellar magnetic field [8].

4 Magnetospheric Turbulence

4.1 Analysis of THEMIS Data in the Earth's Magnetosheath

Naturally, nonlinear structures responsible for turbulence has been already identified in planetary environment, also in the magnetosheath, e.g. [1,34],

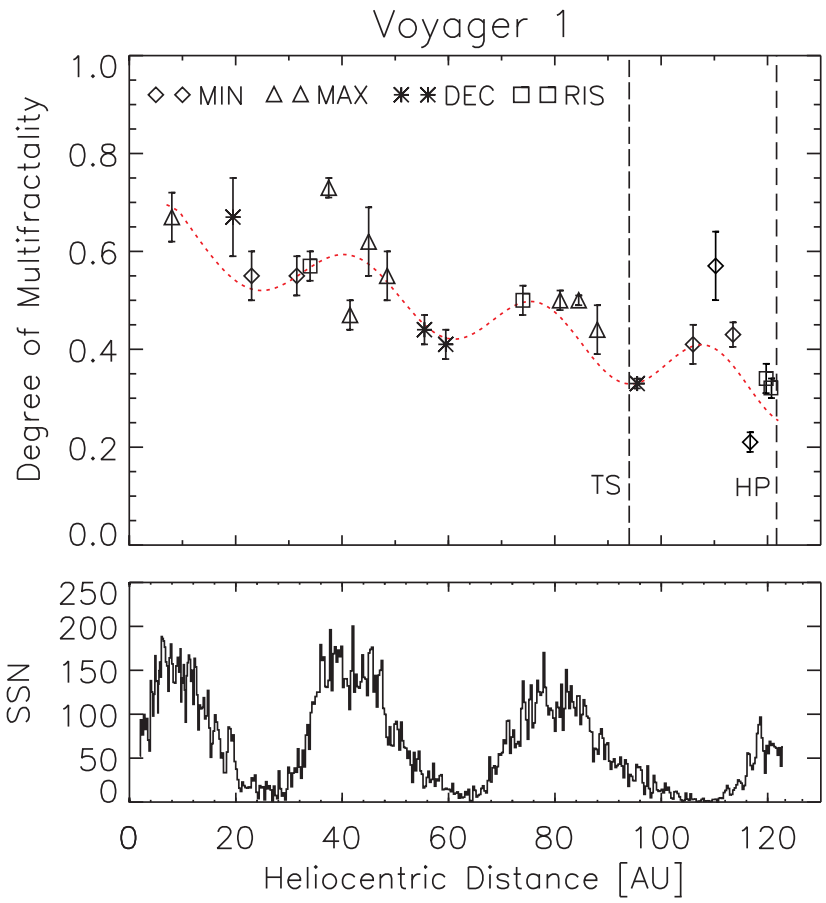

Fig. 3. The degree of multifractality Δ in the heliosphere versus the heliospheric distances.

as illustrated in Fig. 4 [32]. In addition, kinetic simulations have suggested some interesting relation of turbulent processes near shocks to reconnection processes [12]. But in spite of progress in MHD simulations, including Hall effects, the physical mechanisms of turbulent behavior in the magnetosheath are still not sufficiently clear.

4.2 Kurtosis near the Bow Shock

The plasma parameter β, which is the ratio of the thermal pressure p to the magnetic pressure $\mathbf{B}^2/(2\mu_0\rho)$, characterize the plasma with the mass density $\rho = m_i N$ for ions of mass m_i (with $m_i = 1.15\ m_\mathrm{p}$, the proton mass) and the number density N (μ_0 denotes the permeability of free space), while the Alfvén Mach number M_A, the ratio of the ion velocity V to the Alfvén velocity $V_\mathrm{A} = B/(\mu_0\rho)^{1/2}$, is related to the strength of the shock formed in the plasma.

In Ref. [23] we have shown that at very high Alfvénic Mach numbers M_A and high plasma β, i.e. when the thermal pressure dominates the plasma, for the

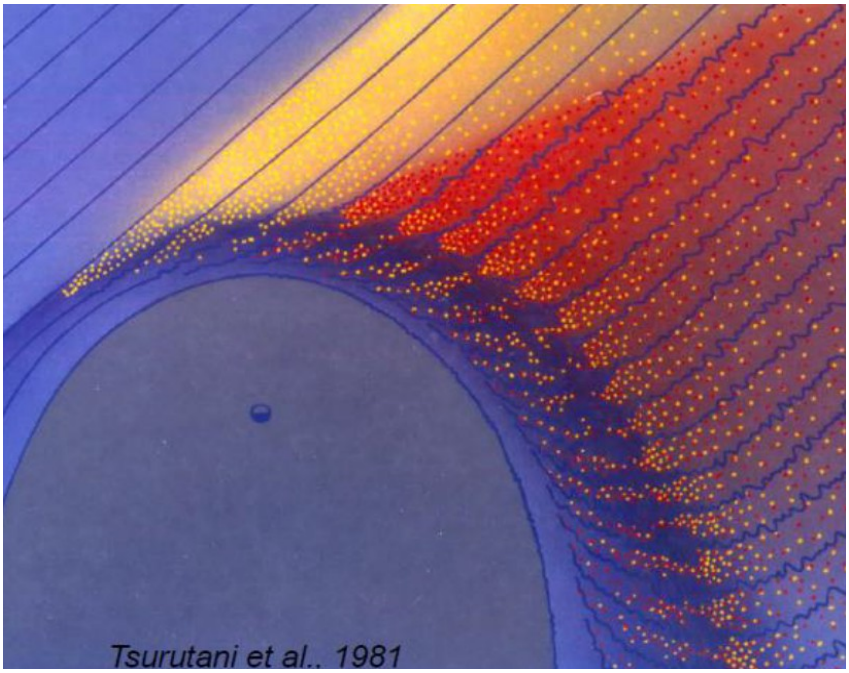

Fig. 4. Turbulence at shocks

direction along the local background magnetic field the probability distribution of compressive fluctuations should be nearly normal and close to equilibrium with small kurtosis, while in the plane perpendicular to the local magnetic field Alfvénic turbulence resulting from nonlinear interactions is non-gyrotropic with large kurtosis for the Elsässer variables $\mathbf{z}^{\pm}$. On the other hand, intermittency becomes somewhat weaker for moderate $M_{\rm A} \sim 10$ (and $\beta \sim 1$). However, the level of intermittency for the outgoing fluctuations ($\mathbf{z}^{+}$) seems to be similar to that for the ingoing fluctuations ($\mathbf{z}^{-}$), which demonstrates equipartition of energy between these oppositely propagating Alfvén waves along the ambient magnetic field.

4.3 Research Hypothesis

The identification of turbulence scaling in the inertial range may not necessarily provide any specific physical mechanism for the multiple processes that are responsible for the distribution of energy or magnetic flux between cascading turbulent eddies. We are convinced that one must consider much smaller scales, where particle-wave interactions resulting in the dissipation of energy are effective, e.g. [1,34].

Hence, our basic research hypothesis is that small scales are essential for understanding of the physical mechanisms of turbulence. In our view, it is necessary to investigate the experimental data at scale lengths below the inertial

range. Moreover, we are convinced that the gross features of turbulence should still be determined by Alfvén waves, e.g. [2], involving the magnetic field and the ion bulk speed of the plasma, possibly related to discontinuities [5], current sheets, mirror mode structures, or instabilities [31].

5 Data from the MMS Mission

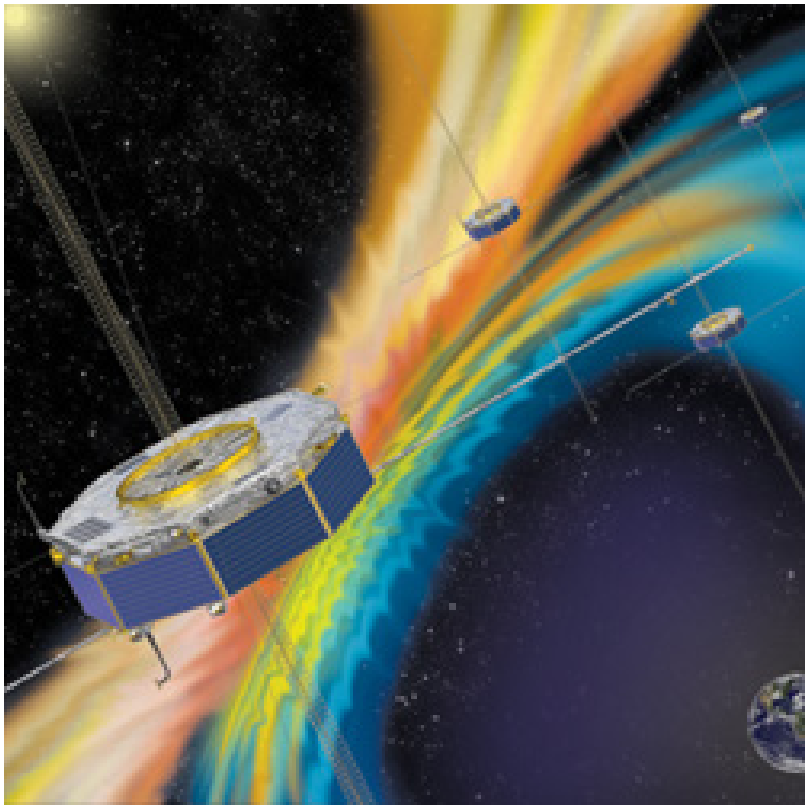

Fig. 5. The *MMS* is a NASA unmanned space mission to study the Earth's magnetosphere, using four identical spacecraft flying in a tetrahedral formation, Credits: NASA.

The *Magnetospheric Multiscale* (*MMS*) mission was launched on 13 March 2015 at 02:44 UTC, as illustrated in Fig. 5. The planned mission duration was 2 years, 5.5 months, but now is in its $5th$ year of operation, and its characteristics are as follows: launch mass: 1,360 kg (2,998 lb); inclination: 28.0° perigee: 2,550 km (1,580 mi) apogee: day phase: 70,080 km (43,550 mi); night phase: 152,900 km (95,000 mi). The location and formation of four spacecraft near the apogee are depicted in Fig. 6 and 7, respectively.

MMS is also equipped with a new navigator based on extremely sensitive GPS equipment to provide absolute position information, Figs. 8 and 9. The

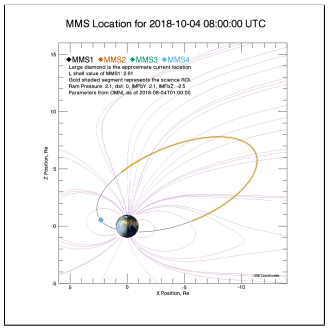

Fig. 6. MMS Location

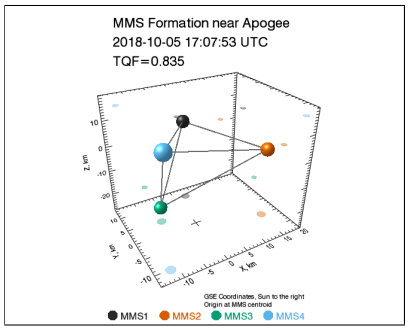

Fig. 7. MMS formation

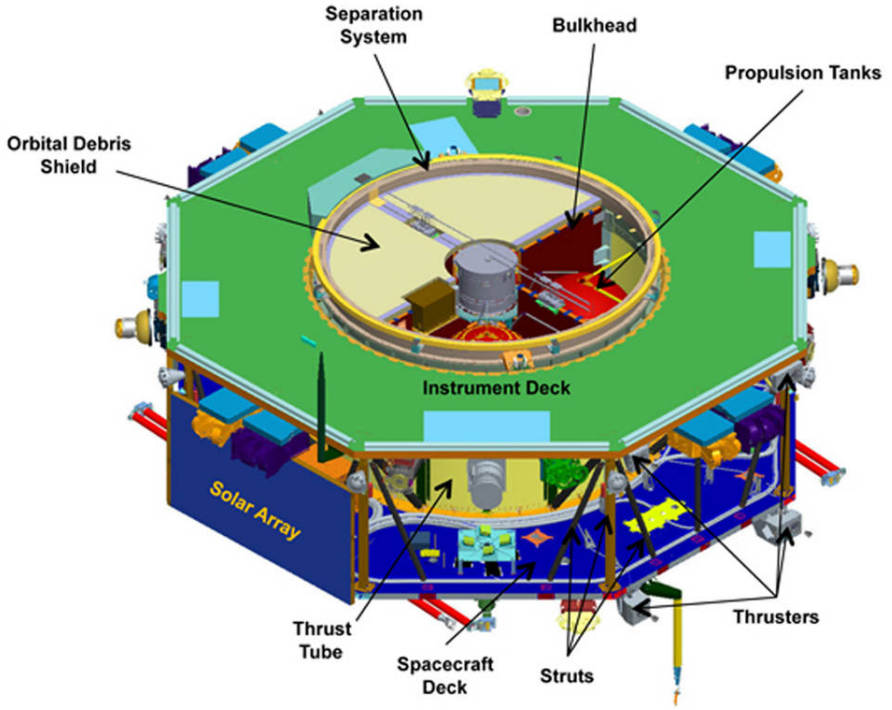

Fig. 8. Illustration of MMS spacecraft with systems labeled, Credits: NASA.

observatories require such sensitive sensors because the satellites fly in an orbit higher than that of the GPS satellites, so they must rely on the weaker signals from GPS satellites on the far side of Earth. The MMS spacecraft were developed at NASA's Goddard Space Flight Center in Greenbelt, MD, USA.

Figure 10 shows the *MMS 1* trajectory in the Geocentric Solar Ecliptic (GSE) coordinates. The dotted–dashed line shows the position of the bow shock, while the solid line shows the magnetopause [17].

MMS data access

https://lasp.colorado.edu/mms/sdc/public/

https://spdf.gsfc.nasa.gov/

FGM	FPI (ions and electrons)
brst: 7.8 milliseconds	brst: 30 milliseconds
srvy: 0.0625 to 0.125 sec	fast: 4.5 seconds

Fig. 9. MMS data access and resolution

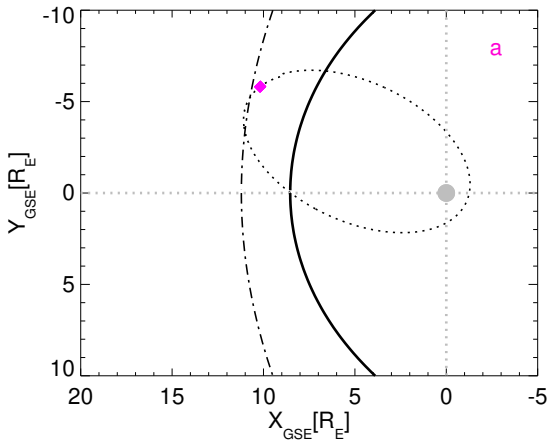

Fig. 10. *MMS 1* spacecraft trajectory in the magnetosheath behind the bow shock.

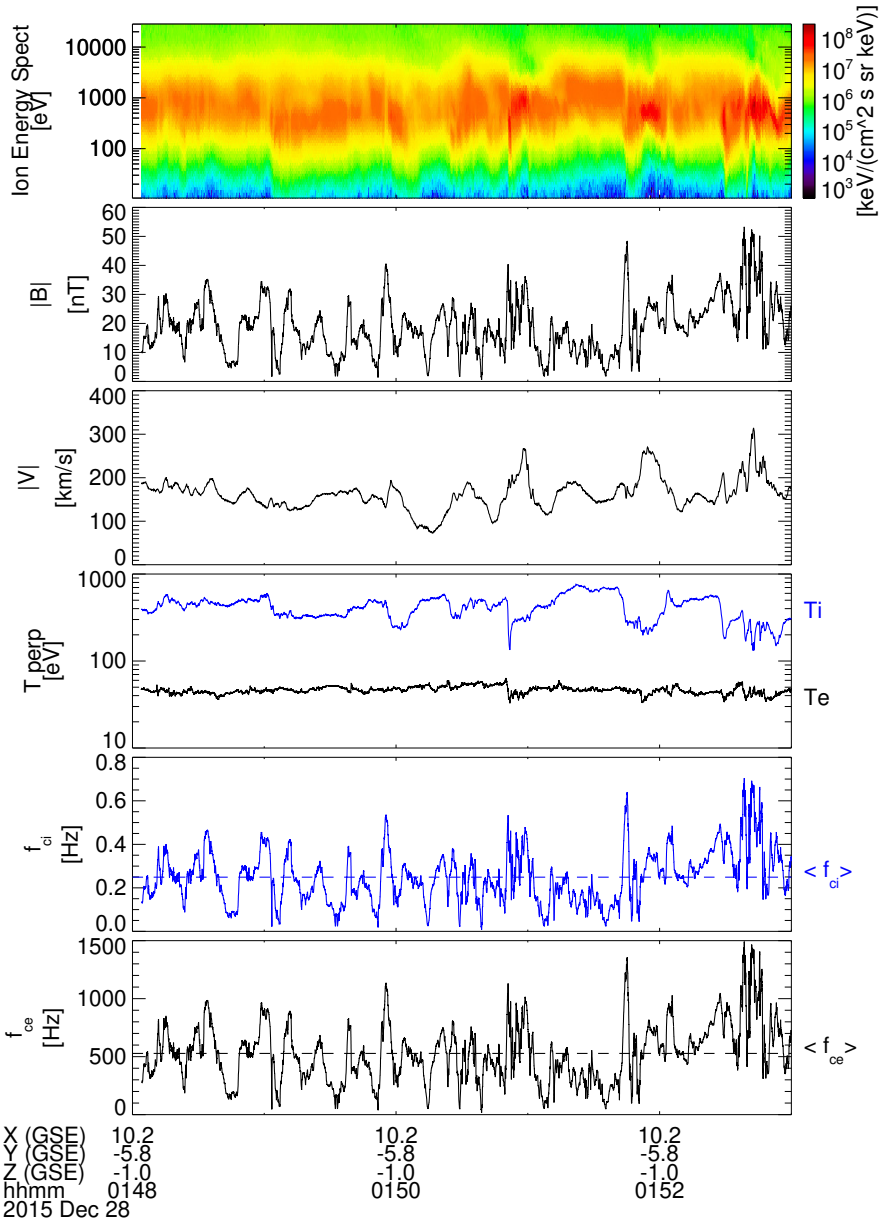

Fig. 11. Data for high-resolution turbulence in the magnetosheath behind the bow shock.

6 Methods of Data Analysis

We have employed a standard statistical analysis to obtain energy density spectra for the magnetic field strength and the ion speed at high time resolution, specified in Fig. 9. This approach is used for estimating the power of signal at various frequencies by using the periodograms resulting from converting any signal from the time domain to the frequency domain. Due to noise reduction in the power spectra this method allows to reduce the frequency resolution.

In a magnetized plasma the ion $\omega_i = 2\pi f_i = (ZeB)/(m_i c)$ (with $Z = 1$) and and electron $\omega_e = 2\pi f_e = (eB)/(m_e c)$ gyrofrequency, which characterize the kinetic regime, depend on the embedded magnetic field strength $|\mathbf{B}|$. The respective Larmor radii are $r_{Li,e} = (V_{\mathrm{th}\perp i,e})/(\omega_{i,e})$, where $V_{\mathrm{th}\perp i,e} = (kT_{\perp i,e}/m_{i,e})^{1/2}$ are the thermal velocities (with the Boltzmann constant k) corresponding to the ion and electron temperatures perpendicular to the local magnetic field, $T_{\perp i}$ and $T_{\perp e}$, respectively. With ion and electron plasma frequencies $\omega_{pi,e} = 2\pi f_{pi,e}$ the ion and electron inertial lengths are $\lambda_{i,e} = c/(\omega_{pi,e})$ (c is the speed of light). Therefore, employing the Taylor's hypothesis the characteristic ion and electron inertial frequencies are $f_{\lambda i,e} = (V/c)\ f_{pi,e}$.

7 Results of Analysis for Magnetosheath Turbulence near the Bow Shock

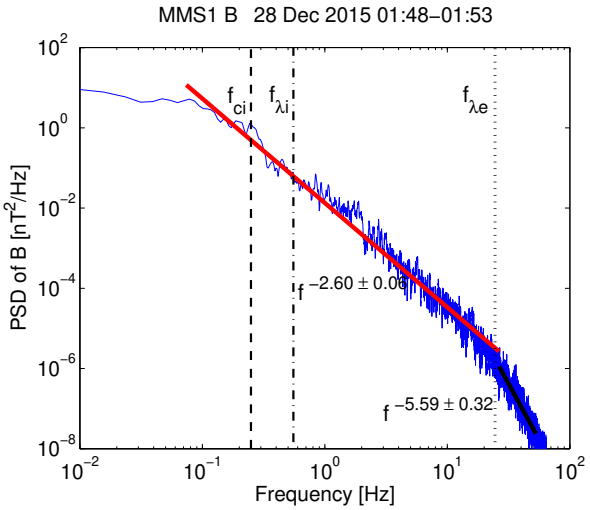

Fig. 12. Energy spectrum for turbulence behind the bow shock.

The magnetosheath can easily be identified based on broad ion energy spectra ranging from 100 eV to a few keV as illustrated for the sample near the bow shock in the first upper panels of Fig. 11. The second and third panels show the magnetic field $|\mathbf{B}|$ and the ion velocity $|\mathbf{V}|$. The fourth panel presents ion

and electron temperatures $T_{\perp i}$ and $T_{\perp e}$, while the fifth and sixth panels show the calculated gyrofrequencies, f_{ci} and f_{ce}, with averages marked by dashed lines. Kinetic scales estimated using the Taylor's hypothesis, approximately span the interval from 1 to 100 km.

Fig. 12 shows the energy spectrum for turbulence behind the bow shock for frequencies above the ion gyrofrequency f_{ci} marked by the dashed vertical line, and between the ion $f_{\lambda i}$ and electron $f_{\lambda e}$ Taylor-shifted inertial frequencies shown by the dashed–dotted and dotted lines, respectively [17]. In this case, near the ion frequency of $f_{ci} = 0.25$ Hz, we have observed a clear change of the spectral exponent of the magnetic spectra from -0.8 to much steeper spectrum with the slope of -5/2, which is substantially different than that for the standard Kolmogorov [13] or Kraichnan [14] spectra with the slope of -5/3 or -3/2, characteristic for an inertial region in the magnetized plasma.

Moreover, just behind the bow shock and also near the magnetopause, as discussed in Ref. [17], the availability of the high-resolution magnetic field data of 7.8 ms enabled us to observe a spectral exponents in the kinetic regime (between 0.1 and 65 Hz) from -5/2 above the ion gyrofrequency till -7/2 or even -11/2 (or -16/3) above the Taylor-shifted frequency related to the electron skin depth $f_{\lambda e}$ of about 20 – 25 Hz (far below $f_{ce} = 528$ Hz). The largest break in the spectral slope of about -16/3 in Fig. 12 could result from the dissipation of the kinetic Alfvén waves, e.g. [26]. This certainly requires further investigation to compare our experimental results with kinetic theory.

Because the plasma resolution for ions is only 150 ms [17], the similar spectrum for the velocity can only be resolved between 0.04 and 3.5 Hz, near the onset of kinetic scales, which is at least inside the magnetosheath similar to the Kolmogorov [13] type with the well-known slope of -5/3.

8 Magnetospheric Conclusions

Using *THEMIS* data we have demonstrated that turbulence is intermittent in the entire magnetosheath, in regions near the bow shock and even near the magnetopause. It seems that turbulence behind the quasi-perpendicular shock is more intermittent with larger kurtosis than behind the quasi-parallel shock.

We have looked at turbulence spectra in regions behind the bow shock and close to the magnetopause, using the highest-resolution data, and also deep inside the magnetosheath, where only lower-resolution data are available.

It is worth noting that the unprecedented very high-resolution (of about 8 milliseconds) of the magnetometer of the *MMS* mission enables us to analyze turbulence on kinetic scale lengths of only tens of kilometers, i.e. extremely small in the space environment. In particular, it has appeared that a clear break of the magnetic spectrum exponent to about -11/2 at the electron inertial frequencies $f_{\lambda e} = 20$–25 Hz agrees with the predictions of kinetic theory (-16/3).

In view of the current and forthcoming space investigations, we expect that our study on the difference in characteristic of energy spectral density can help facilitate a better understanding of the physical processes after applying kinetic theory for turbulence in various regions of space and astrophysical plasmas.

Acknowledgments. We are grateful for the dedicated efforts of the entire *Voyager*, *THEMIS*, and *MMS* mission teams, including development, science operations, and the Science Data Center at the University of Colorado. We especially benefited from the efforts of J. L. Burch, L. F. Burlaga, D. G. Sibeck, and C. T. Russells for providing the data that are available online from http://cdaweb.gsfc.nasa.gov. This work has been supported by the National Science Center, Poland (NCN), through grant 2014/15/B/ST9/04782, and from the *MMS* project through the Catholic University of America during a visit by W.M.M to the NASA Goddard Space Flight Center.

References

1. O. Alexandrova. Solar wind vs magnetosheath turbulence and Alfvén vortices. *Nonlinear Processes Geophys.*, 15(1):95–108, 2008.
2. J. W. Belcher and Jr. Davis, L. Large-amplitude alfvén waves in the interplanetary medium, 2. *J. Geophys. Res.*, 76(16):3534–3563, 1971.
3. D. Biskamp. *Magnetic Reconnection in Plasmas*, volume 3 of *Cambridge monographs on plasma physics*. Cambridge, UK: Cambridge University Press, 2000.
4. D. Biskamp. *Magnetohydrodynamic Turbulence*. Cambridge, UK: Cambridge University Press, 2003.
5. J. E. Borovsky. Contribution of strong discontinuities to the power spectrum of the solar wind. *Phys. Rev. Lett.*, 105:111102, 2010.
6. R. Bruno and V. Carbone. *Turbulence in the Solar Wind*, volume 928 of *Lecture Notes in Physics*. Springer International Publishing, Berlin, 2016.
7. L. F. Burlaga. *Interplanetary Magnetohydrodynamics*. New York: Oxford University Press, 1995.
8. L. F. Burlaga and N. F. Ness. Voyager 1 observations of the interstellar magnetic field and the transition from the heliosheath. *Astrophys. J.*, 784:146, 2014.
9. K. Falconer. *Fractal Geometry: Mathematical Foundations and Applications*. J. Wiley: New York, 1990.
10. P. Figura and W. M. Macek. Model of line preserving field line motions using Euler potentials. *Annals of Physics*, 333:127–135, 2013.
11. U. Frisch. *Turbulence. The Legacy of A.N. Kolmogorov*. Cambridge Univ. Press: Cambridge, 1995.
12. H. Karimabadi, V. Roytershteyn, H. X. Vu, Y. A. Omelchenko, J. Scudder, W. Daughton, A. Dimmock, K. Nykyri, M. Wan, D. Sibeck, M. Tatineni, A. Majumdar, B. Loring, and B. Geveci. The link between shocks, turbulence, and magnetic reconnection in collisionless plasmas. *Phys. Plasmas*, 21(6):062308, 2014.
13. A. Kolmogorov. The local structure of turbulence in incompressible viscous fluid for very large Reynolds' numbers. *Dokl. Akad. Nauk SSSR*, 30:301–305, 1941.
14. R. H. Kraichnan. Inertial-range spectrum of hydromagnetic turbulence. *Phys. Fluids*, 8:1385–1387, 1965.
15. W. Macek and S. Grzedzielski. Earth, Jupiter and Sun - similarity of plasma transport across the cavity boundaries. In B. McNamara, editor, *Twenty Years of Plasma Physics*, pages 320–327. World Scientific: Singapure, 1985.
16. W. M. Macek. Multifractality and intermittency in the solar wind. *Nonlinear Processes Geophys.*, 14:695–700, 2007.
17. W. M. Macek, A. Krasińska, M. V. D. Silveira, D. G. Sibeck, A. Wawrzaszek, J. L. Burch, and C. T. Russell. Magnetospheric multiscale observations of turbulence in the magnetosheath on kinetic scales. *Astrophys. J. Lett.*, 864(2):L29, 2018.

18. W. M. Macek and A. Szczepaniak. Generalized two-scale weighted Cantor set model for solar wind turbulence. *Geophys. Res. Lett.*, 35, 2008.
19. W. M. Macek and A. Wawrzaszek. Evolution of asymmetric multifractal scaling of solar wind turbulence in the outer heliosphere. *J. Geophys. Res.*, 114(13), 2009.
20. W. M. Macek, A. Wawrzaszek, and L. F. Burlaga. Multifractal structures detected by Voyager 1 at the heliospheric boundaries. *Astrophys. J. Lett.*, 793:L30, 2014.
21. W. M. Macek, A. Wawrzaszek, and V. Carbone. Observation of the multifractal spectrum at the termination shock by Voyager 1. *Geophys. Res. Lett.*, 38:L19103, 2011.
22. W. M. Macek, A. Wawrzaszek, and V. Carbone. Observation of the multifractal spectrum in the heliosphere and the heliosheath by Voyager 1 and 2. *J. Geophys. Res.*, 117:12101, 2012.
23. W. M. Macek, A. Wawrzaszek, B. Kucharuk, and D. G. Sibeck. Intermittent anisotropic turbulence detected by themis in the magnetosheath. *Astrophys. J. Lett.*, 851(2):L42, 2017.
24. C. Meneveau and K. R. Sreenivasan. Simple multifractal cascade model for fully developed turbulence. *Phys. Rev. Lett.*, 59:1424–1427, 1987.
25. E. Ott. *Chaos in Dynamical Systems*. Cambridge Univ. Press: Cambridge, 1993.
26. A. A. Schekochihin, S. C. Cowley, W. Dorland, G. W. Hammett, G. G. Howes, E. Quataert, and T. Tatsuno. Astrophysical gyrokinetics: Kinetic and fluid turbulent cascades in magnetized weakly collisional plasmas. *Astrophys. J. Supp.*, 182:310–377, 2009.
27. M. Strumik, A. Czechowski, S. Grzedzielski, W. M. Macek, and R. Ratkiewicz. Small-scale local phenomena related to the magnetic reconnection and turbulence in the proximity of the heliopause. *Astrophys. J. Lett.*, 773:L23, 2013.
28. M. Strumik, S. Grzedzielski, A. Czechowski, W. M. Macek, and R. Ratkiewicz. Advective transport of interstellar plasma into the heliosphere across the reconnecting heliopause. *Astrophys. J. Lett.*, 782:L7, 2014.
29. R. A. Treumann. Fundamentals of collisionless shocks for astrophysical application, 1. Non-relativistic shocks. *Astronom. Astrophys. Rev.*, 17:409–535, 2009.
30. R. A. Treumann and W. Baumjohann. Collisionless magnetic reconnection in space plasmas. *Frontiers in Physics*, 1:31, 2013.
31. B. T. Tsurutani, G. S. Lakhina, O. P. Verkhoglyadova, E. Echer, F. L. Guarnieri, Y. Narita, and D. O. Constantinescu. Magnetosheath and heliosheath mirror mode structures, interplanetary magnetic decreases, and linear magnetic decreases: Differences and distinguishing features. *J. Geophys. Res.*, 116:2103, 2011.
32. B. T. Tsurutani and P. Rodriguez. Upstream waves and particles: An overview of ISEE results. *J. Geophys. Res.*, 86(A6):4317–4324, 1981.
33. V. M. Vasyliunas. Theoretical models of magnetic field line merging. I. *Rev. Geophys. Space Phys.*, 13:303–336, 1975.
34. E. Yordanova, A. Vaivads, M. André, S. C. Buchert, and Z. Vörös. Magnetosheath plasma turbulence and its spatiotemporal evolution as observed by the Cluster spacecraft. *Phys. Rev. Lett.*, 100(20):205003, 2008.